This article was downloaded by:
On: *21 January 2011*
Access details: *Access Details: Free Access*
Publisher *Taylor & Francis*
Informa Ltd Registered in England and Wales Registered Number: 1072954 Registered office: Mortimer House, 37-41 Mortimer Street, London W1T 3JH, UK

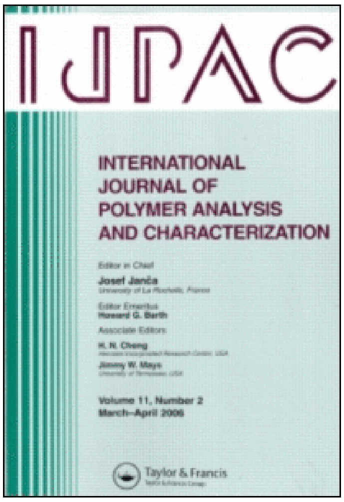

International Journal of Polymer Analysis and Characterization
Publication details, including instructions for authors and subscription information:
http://www.informaworld.com/smpp/title~content=t713646643

Structure, Thermal, and Antibacterial Properties of Polyacrylonitrile/Ferric Chloride Nanocomposite Fibers by Electrospinning

Yibing Cai[ab]; Qingqing Wang[a]; Qufu Wei[a]; Qin You[a]; Fenglin Huang[a]; Lei Song[b]; Yuan Hu[b]; Weidong Gao[a]
[a] Key Laboratory of Eco-textiles, Ministry of Education, Jiangnan University, Wuxi, Jiangsu, China [b] State Key Laboratory of Fire Science, University of Science and Technology of China, Hefei, Anhui, China

Online publication date: 01 February 2010

To cite this Article Cai, Yibing , Wang, Qingqing , Wei, Qufu , You, Qin , Huang, Fenglin , Song, Lei , Hu, Yuan and Gao, Weidong(2010) 'Structure, Thermal, and Antibacterial Properties of Polyacrylonitrile/Ferric Chloride Nanocomposite Fibers by Electrospinning', International Journal of Polymer Analysis and Characterization, 15: 2, 110 — 118

To link to this Article: DOI: 10.1080/10236660903525083

URL: http://dx.doi.org/10.1080/10236660903525083

PLEASE SCROLL DOWN FOR ARTICLE

Full terms and conditions of use: http://www.informaworld.com/terms-and-conditions-of-access.pdf

This article may be used for research, teaching and private study purposes. Any substantial or systematic reproduction, re-distribution, re-selling, loan or sub-licensing, systematic supply or distribution in any form to anyone is expressly forbidden.

The publisher does not give any warranty express or implied or make any representation that the contents will be complete or accurate or up to date. The accuracy of any instructions, formulae and drug doses should be independently verified with primary sources. The publisher shall not be liable for any loss, actions, claims, proceedings, demand or costs or damages whatsoever or howsoever caused arising directly or indirectly in connection with or arising out of the use of this material.

International Journal of Polymer Anal. Charact., 15: 110–118, 2010
Copyright © Taylor & Francis Group, LLC
ISSN: 1023-666X print
DOI: 10.1080/10236660903525083

Downloaded At: 15:21 21 January 2011

STRUCTURE, THERMAL, AND ANTIBACTERIAL PROPERTIES OF POLYACRYLONITRILE/FERRIC CHLORIDE NANOCOMPOSITE FIBERS BY ELECTROSPINNING

**Yibing Cai,[1,2] Qingqing Wang,[1] Qufu Wei,[1] Qin You,[1]
Fenglin Huang,[1] Lei Song,[2] Yuan Hu,[2] and Weidong Gao[1]**
[1]*Key Laboratory of Eco-textiles, Ministry of Education, Jiangnan University, Wuxi, Jiangsu, China*
[2]*State Key Laboratory of Fire Science, University of Science and Technology of China, Hefei, Anhui, China*

In the present work, the manufacturing of pure polyacrylonitrile (PAN) nanofiber and PAN/$FeCl_3$ nanocomposite fibers was explored by an electrospinning process. The effects of $FeCl_3$ on the structure, thermal stability, and antibacterial properties of the PAN nanocomposite fibers were studied, and were respectively characterized by scanning electron microscopy (SEM), thermogravimetric analyses (TGA), and shake flask tests. The SEM images showed that the diameters of nanocomposite fibers decreased with the loading of $FeCl_3$. The TGA analyses revealed that the onset temperature of thermal decomposition, maximum decomposition temperature, and amount of charred residue at 700°C of PAN nanocomposite fibers was notably increased in the presence of $FeCl_3$, contributing to improved thermal stability properties. It was also found that the reduction percentage of the tested bacteria, Escherichia coli, reached 87% when the $FeCl_3$ content was 5 wt.% of the PAN nanocomposite fibers.

Keywords: Antibacterial properties; Electrospinning; PAN/$FeCl_3$ nanocomposite fibers; Structure; Thermal stability

INTRODUCTION

Nanofibers have attracted a great deal of attention due to their remarkable properties, such as light weight, small diameters, controllable pore structures, and high surface-to-volume ratio, compared to the other conventional fibrous structures.

Submitted 19 October 2009; accepted 25 November 2009.

The work was financially supported by the Open Project Program of State Key Laboratory of Fire Science, University of Science and Technology of China (No. HZ2009KF06), the Program for New Century Excellent Talents in University (No. NCET-06-0485), the Research Fund for the Doctoral Program of Higher Education of China (No. 200802951011), the Natural Science Initial Research Fund of Jiangnan University (No. 2008LYY002), the Self-determined Research Program of Jiangnan University (No. JUSRP20903), and the Open Project Program of Key Laboratory of Eco-Textiles, Ministry of Education, Jiangnan Univeristy (No. KLET0909).

Correspondence: Qufu Wei and Fenglin Huang, Key Laboratory of Eco-textiles, Ministry of Education, Jiangnan University, Wuxi, 214122, Jiangsu, China. E-mail: qfwei@jiangnan.edu.cn; windhuang325@163.com

These properties make nanofibers ideal for use in such application areas as filtration, sensors, protective clothing, tissue engineering, and functional materials.[1–5] Electrospinning is currently one of the most versatile and promising processes for producing continuous nanofibers for both fundamental and application-oriented research, due to its capability and feasibility in generating large quantities of nanofibers. In the electrospinning process, a thin polymer jet is ejected when the electrostatic force applied to the droplets of polymer solutions overcomes the liquid surface tension. The charged jet is elongated and accelerated by the electrostatic field, undergoing stretching, solvent evaporation, and deposition on a substrate as a random fibrous web.[3,4]

Recently, much work has focused on the dispersion of nanoparticles or inorganic salts into electrospun polymer nanofibers due to the fact that such nanofibers allow a unique blend of properties, such as good mechanical strength and heat stability of inorganic materials and excellent flexibility and moldability of polymers, while they still can maintain other functional properties of either constituent. Among various polymer/inorganic composite nanofibers, the used nanoparticles or inorganic salts included montmorillonite (MMT),[1–5] Ag,[6] TiO_2[7] SiO_2,[8–10] Fe_3O_4,[11] silicon nitride (Si_3N_4),[12] $ZnCl_2$,[13] and ferric acetylacetonate ($Fe(acac)_2$).[14]

Downloaded At: 15:21 21 January 2011

In the present work, we report the incorporation of ferric chloride ($FeCl_3$) salts into electrospun polymer nanofibers to form a new type of functional material. $FeCl_3$ is an important transition metal halide that is often used as a Lewis acid. Lewis acids represent a wide range of chemical substances that are able to accept an electron pair and create a coordinate bond. It is known that some polymers with strongly electronegative groups (e.g., –CN) can coordinate Lewis acids, and this may change the polymer degradation mechanism. Lewis acid-type transition metal chlorides can also act as effective cross-linking catalysts.[15–17] Additionally, $FeCl_3$ still has a sterilization function and is an effective flocculant for sewage treatment. Current research efforts have focused on the fabrication, structure morphology, and thermal stability properties of $FeCl_3$-added PAN nanofibers and their response to the tested bacteria, *Escherichia coli*.

EXPERIMENTAL SECTION

Materials

The polyacrylonitrile (PAN, $Mw = 79,100\,g/mol$) powder was obtained from Aldrich and used without further purification. The ferric chloride ($FeCl_3 \cdot 6H_2O$) was obtained from the Shanghai Chemical Regents Company. The 99.5% N,N-dimethyl formamide (DMF) was used as received. All chemicals were analytical grade and were used as received without further purification.

Fabrication of Electrospun Nanocomposite Fibers

DMF solutions of PAN (12 wt.%) containing various amounts of $FeCl_3$ (0, 1, 3, and 5 wt.%) were prepared. Mechanical stirring was applied for at least 24 h to form homogeneous solutions. Electrospinning solutions were loaded in a 10 mL syringe with a stainless steel capillary metal-hub needle. The inner diameter of the metal needle was 0.30 mm. The positive electrode of the high-voltage power supply was connected to the needle tip. The grounded electrode was connected to a metallic collector covered with aluminum foil. The positive voltage, working distance, and flow rate were respectively fixed at 14 kV, 15 cm (the distance between the needle tip and the collection plate), and 0.4 mL/h. Under high voltage, a polymer jet was ejected and accelerated toward the counter electrode, during which the solvent was rapidly evaporated. Dry nanofibers accumulated on the surface of the aluminum foil and were collected as a fibrous web.

Antibacterial Test

The antibacterial effect was investigated using the shake flask test in accordance with the Chinese national standard GB15979-2002 (hygienic standard for disposable sanitary products). The used bacteria were *Escherichia coli*. In addition to the PAN/$FeCl_3$ nanocomposite fiber film, pure PAN nanofiber film was also tested for comparison. After incubation at 37 ± 1°C for 36 h, bacteria were counted.

The antibacterial property of the PAN/$FeCl_3$ nanocomposite fiber film was evaluated by calculating the reduction percentage of bacteria by the following formula:

$$Xs = (A - B)/A$$

where Xs is the reduction percentage of bacteria, %; A is the number of bacteria colonies on the agar plate recovered from bacterial solution at 0 contact time; and B is the number of bacteria colonies on the agar plate recovered from the specimen after shaking for 1 h. If the number of the bacteria after shaking was larger than the number at 0 contact time, $Xs = 0$.

Characterization

A scanning electron microscope (SEM, SU-1510) was used to examine the structures of the nanocomposite fibers. The samples were coated with a thin layer of gold by sputtering before the SEM imaging. An accelerating voltage of 15 kV with accounting time of 100 s was applied.

Thermogravimetric analyses (TGA) were carried out using a TGA50H thermo-analyzer instrument at temperatures from 25° to 700°C using a linear heating rate of 10°C/min under nitrogen flow. The nitrogen flow was 25 mL/min. Samples were measured in a sealed alumina pan with a mass of about 10 mg. The temperature and mass reproducibility of the instrument were ±2.0°C and ±2.0%, respectively.

RESULTS AND DISCUSSION

Structure and Morphology

The SEM images of electrospun PAN nanofibers and PAN/$FeCl_3$ nanocomposite fibers, collected on the aluminum foil, are illustrated in Figure 1.

Downloaded At: 15:21 21 January 2011

Downloaded At: 15:21 21 January 2011

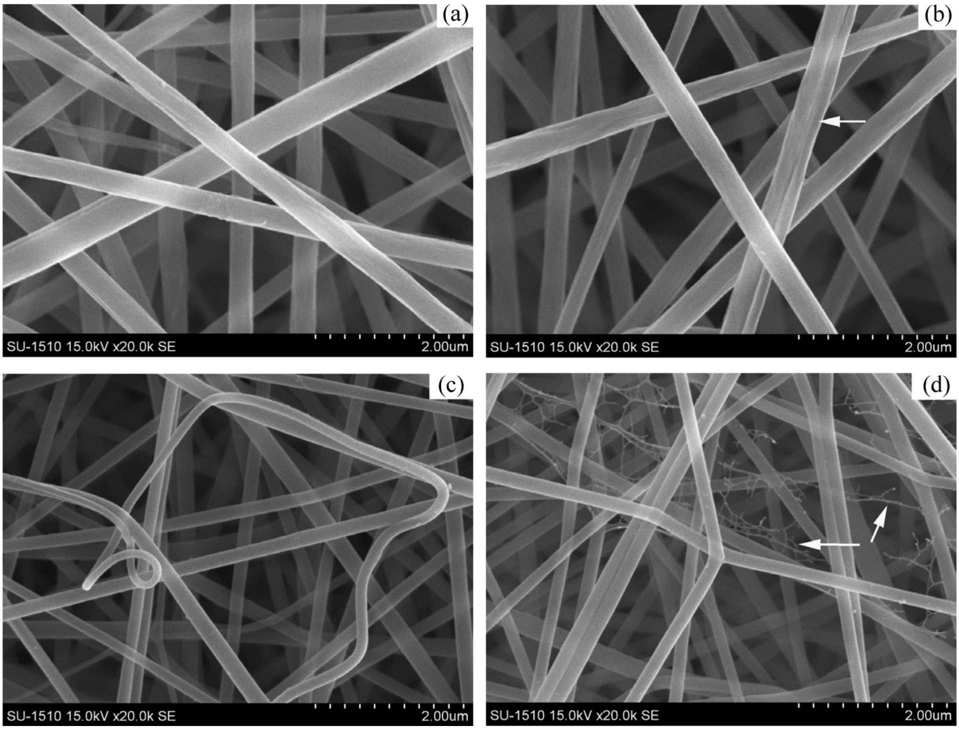

Figure 1. SEM images of (a) PAN nanofibers, (b), (c), and (d) PAN nanocomposite fibers with 1 wt.%, 3 wt.%, and 5 wt.% $FeCl_3$.

The nanofibers were randomly distributed to form the fibrous web. It was observed that the electrospun nanofibers had variable fiber diameters. The morphology and average diameter of the electrospun PAN/$FeCl_3$ nanocomposite fibers were significantly affected by the amount of $FeCl_3$ added. Figure 1(a) shows that the average diameters of the PAN nanofibers ranged from about 250 to 400 nm. However, the average diameter of the PAN/$FeCl_3$ nanocomposite fibers was less than those of the PAN nanofibers. The average diameter of electrospun PAN nanocomposite fibers with 1 wt.% $FeCl_3$ was approximately 200–300 nm, with better homogeneous distribution. It could be also found that some nanofibers adhered to other nanofibers, as indicated by the arrow in Figure 1(b). As shown in Figure 1(c), the average diameter of nanocomposite fibers was further decreased to 100–200 nm, with an extremely homogeneous distribution, when the amount of the $FeCl_3$ was increased to 3 wt.%. The almost uniform nanofiber diameters, of about 150 nm, for PAN nanocomposite fibers with 5 wt.% $FeCl_3$ were observed. Meanwhile, secondary nanofibers with several nanometer diameters were also found, as indicated by arrows in Figure 1(d).

The loading of inorganic salts ($FeCl_3$) increased the charge density in ejected jets, and thus stronger elongation forces were imposed to the jets because of the self-repulsion of the excess charges under the electrical field, resulting in substantially straighter shape and smaller diameter of electrospun fibers. Meanwhile, the conductivity of the PAN composite solution was also another major factor affecting the morphology and diameter of the electrospun PAN nanofibers. The Fe^{3+} ions derived from inorganic salts improved the conductivity of PAN/$FeCl_3$ solutions. In addition, solution conductivity increased with increasing $FeCl_3$ concentration since more free ions were available.[2,4,13,18–20] Therefore, the decrease of nanofiber diameter with increasing $FeCl_3$ concentration should be attributed predominantly to the increased conductivity of the polymer solutions.

Thermal Stability Properties

It is well known that the inorganic salt $FeCl_3$ is a kind of Lewis acid and could act as an effective cross-linking catalyst. Additionally, it could change the polymer degradation mechanism, and it could coordinate with strongly electronegative groups (e.g., –CN).[15–17] Therefore, in the present work, the influence of $FeCl_3$ on the thermal stability properties of PAN nanocomposite fibers was studied by thermogravimetric analysis (TGA). The TGA and differential thermogravimetric analysis (DTGA) curves of pure PAN nanofibers and PAN nanocomposite fibers with different $FeCl_3$ amounts are shown in Figures 2 and 3, respectively. The 5% weight loss temperature ($T_{-5\,wt\%}$), the maximum decomposition temperature (T_{max1} and T_{max2}), and the charred residue at 700°C are listed in Table I. It can be seen from the TGA and DTGA curves that there are two-step degradation processes for both pure PAN nanofibers and PAN/$FeCl_3$ nanocomposite fibers. The results indicate that the onset of degradation and maximum decomposition for the PAN/$FeCl_3$ nanocomposite fibers occurs at higher temperatures than for the pure PAN nanofibers. The degradation temperature of 5 wt.% weight loss for the PAN/$FeCl_3$ nanocomposite fibers increased from 271.4°C for the pure PAN nanofibers to 295.1°C (PAN/1 wt.% $FeCl_3$), 301.1°C (PAN/3 wt.% $FeCl_3$),

Downloaded At: 15:21 21 January 2011

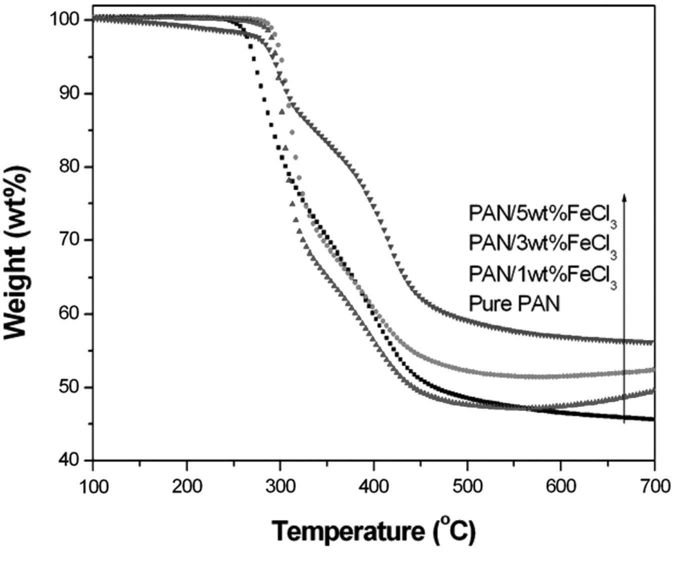

Figure 2. TGA curves of pure PAN nanofibers and PAN/$FeCl_3$ nanocomposite fibers.

Downloaded At: 15:21 21 January 2011

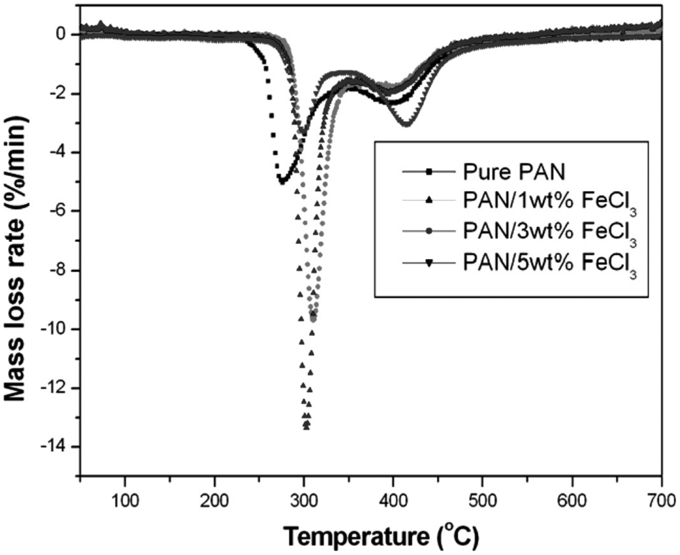

Figure 3. DTGA curves of pure PAN nanofibers and PAN/FeCl$_3$ nanocomposite fibers.

and 292.1°C (PAN/5 wt.% FeCl$_3$). The T_{max1} for the PAN/FeCl$_3$ nanocomposite fibers increased to 303.1°C (PAN/1 wt.% FeCl$_3$), 310.5°C (PAN/3 wt.% FeCl$_3$), and 299.6°C (PAN/5 wt.% FeCl$_3$) from 276.8°C for the pure PAN nanofibers. The reasons may be that the FeCl$_3$ is able to create a coordinate bond with strongly electronegative groups (e.g., electronegative nitrogen atom in –CN group). It could attack PAN at acrylonitrile sites at elevated temperatures and lead to the formation of cross-linking.[15] The catalytic properties of the Fe^{3+} would promote the cross bonding of PAN and form charred residue, which would prevent the nanocomposites from decomposing. Meanwhile, the Fe ion is also the operative site for radical trapping and increased thermal stability of PAN nanocomposite fibers.[21]

It could be also found that the $T_{-5wt\%}$ and T_{max1} for PAN nanocomposite fibers with 5 wt.% FeCl$_3$ are slightly lower than those values for the PAN nanocomposite fibers with 1 wt.% and 3 wt.% FeCl$_3$, as shown in Table I. The reasons may be that the excessive FeCl$_3$ sublimed during the thermal degradation, and the effect of FeCl$_3$ on catalysis degradation of PAN is dominant compared to its cross-linking effects.

Table I. TGA data of pure PAN nanofibers and PAN/FeCl$_3$ nanocomposite fibers

Samples	$T_{-5wt\%}$ (°C)	T_{max1} (°C)	T_{max2} (°C)	Charred residue (700°C)
PAN	271.4	276.8	399.6	45.6
PAN/1 wt.% FeCl$_3$	295.1	303.1	398.2	49.6
PAN/3 wt.% FeCl$_3$	301.1	310.5	397.5	52.4
PAN/5 wt.% FeCl$_3$	292.1	299.6	415.6	56.2

It could be also found from Figure 3 and Table I that the yield of charred residue at 700°C for the PAN/$FeCl_3$ nanocomposite fibers is higher than that of pure PAN nanofibers, and the yield of charred residue markedly increased with the increasing $FeCl_3$ amount. The results also show that the addition of 5 wt.% $FeCl_3$ to polyacrylonitrile causes an increase in the amount of charred residue that is nonvolatile at 700°C from 45.6% to 56.2% in nitrogen, implying the interacting behavior of polyacrylonitrile and $FeCl_3$. The reasons may be that the metal atoms (e.g., Fe^{3+}) are coordinately bonded to the strongly electronegative cyano groups of the PAN polymer. The interactions promoted the dehydrogenation of polymer, and these unsaturated sites then led to molecular cross-linking and the formation of nonvolatile charred residue.[15]

It is also known that transition metal halide could thermally loose a halogen atom through a reversible oxidative-reductive catalytic process between Fe^{3+} and Fe^{2+}. This reaction should be accelerated by the additional coordination to the cyano groups. The liberated halogen atom may remove a hydrogen atom from the main chain of the PAN and leave a radical site on the PAN chains. These carbon-centered macroradicals could undergo the process of radical recombination, leading to direct cross-linking via coupling pathway. Therefore, the dehydrogenation (leading to macroradical formation) and recombination of the macroradicals (leading to intermolecular cross-linking) by transition metal chlorides may be the key steps in the formation of charred residue for the PAN nanocomposite fibers. In other words, it was believed that the transition metal chlorides delayed the escape of pyrolytic products and initiated the formation of macroradicals during thermal degradation and thus led to radical recombination and intermolecular cross-linking.[15,16,22] Additionally, the Fe ion could capture the radicals during the thermal degradation of the nanocomposite fibers via gas-phase flame-retardant mechanism.[21] The increased charred residue amount contributed to the improved thermal stability of the PAN nanocomposite fibers.

Downloaded At: 15:21 21 January 2011

Antibacterial Property

The antibacterial performance of the pure PAN nanofiber film and PAN nanocomposite fiber film with 5 wt.% $FeCl_3$ was measured by the shake flask test. The test results are listed in Table II. The pure PAN nanofiber film was not effective against *Escherichia coli* since the percent reduction of bacteria was 0. However, the PAN nanocomposite fiber film was very effective against test bacteria with a

Table II. Antibacterial results by shake flask tests

	Concentration (diluted times)				
Samples	$\times 10^0$	$\times 10^1$	$\times 10^2$	$\times 10^3$	Percent reduction of bacteria
Blank	>300	>300	124	127	–
PAN	>300	>300	125	135	0.00
PAN/$FeCl_3$[a]	>300	>300	16	7	87.0

[a] PAN nanocomposite fibers with 5 wt.% $FeCl_3$.

reduction of about 87% for *Escherichia coli* (the result based on the concentration diluted 100 times), indicating excellent antibacterial property of $FeCl_3$.

CONCLUSIONS

In the present work, PAN/$FeCl_3$ nanocomposite fibers were prepared by a facile compounding and electrospinning technique. The structures, thermal stability, and antibacterial properties of the electrospun nanocomposite fibers were respectively investigated by SEM, TGA, and shake flask tests. The SEM images showed that the diameters of nanocomposite fibers decreased with increasing $FeCl_3$ amount, due to increased conductivity of the composite solution. The TGA analyses indicated that the increased onset thermal degradation temperature, maximum decomposition temperature, and charred residue amount contributed to improved thermal stability properties of PAN/$FeCl_3$ nanocomposite fibers, attributed to the dehydrogenation and recombination of the macroradicals, thus cross-linking and aromatization to form charred residue. It was also found from the shake flask tests that the reduction percentage of tested bacteria *Escherichia coli* reached 87% for the PAN nanocomposite fibers with 5 wt.% $FeCl_3$, due to the sterilization effects of the transition metal halide $FeCl_3$.

Downloaded At: 15:21 21 January 2011

REFERENCES

1. Fong, H., W. D. Liu, C. S. Wang, and R. A. Vaia. (2002). Generation of electrospun fibers of nylon 6 and nylon 6-montmorillonite nanocomposite. *Polymer* **43**, 775–780.
2. Hong, J. H., E. H. Jeong, H. S. Lee, D. H. Baik, S. W. Seo, and J. H. Youk. (2005). Electrospinning of polyurethane/organically modified montmorillonite nanocomposites. *J. Polym. Sci. Polym. Phys.* **43**, 3171–3177.
3. Wang, M., A. J. Hsieh, and G. C. Rutledge. (2005). Electrospinning of poly(MMA-co-MAA) copolymers and their layered silicate nanocomposites for improved thermal properties. *Polymer* **46**, 3407–3418.
4. Li, L., L. M. Bellan, H. G. Craighead, and M. W. Frey. (2006). Formation and properties of nylon-6 and nylon-6/montmorillonite composite nanofibers. *Polymer* **47**, 6208–6217.
5. Kim, G. M., G. H. Michler, F. Ania, and F. J. Balta Calleja. (2007). Temperature dependence of polymorphism in electrospun nanofibres of PA6 and PA6/clay nanocomposite. *Polymer* **48**, 4814–4823.
6. Wang, Y. Z., Q. B. Yang, G. Y. Shan, C. Wang, J. S. Du, S. G. Wang, Y. X. Li, X. S. Chen, X. B. Jing, and Y. Wei. (2005). Preparation of silver nanoparticles dispersed in polyacrylonitrile nanofiber film spun by electrospinning. *Mater. Lett.* **59**, 3046–3049.
7. Im, J. S., M. I. Kim, and Y. S. Lee. (2008). Preparation of PAN-based electrospun nanofiber webs containing TiO_2 for photocatalytic degradation. *Mater. Lett.* **62**, 3652–3655.
8. Ji, L. W., and X. W. Zhang. (2008). Ultrafine polyacrylonitrile/silica composite fibers via electrospinning. *Mater. Lett.* **62**, 2161–2164.
9. Jung, H. R., D. H. Ju, W. J. Lee, X. W. Zhang, and R. Kotek. (2009). Electrospun hydrophilic fumed silica/polyacrylonitrile nanofiber-based composite electrolyte membranes. *Electrochim. Acta* **54**, 3630–3637.
10. Ding, Y. H., P. Zhang, Y. Jiang, F. Xu, J. R. Yin, and Y. D. Zuo. (2009). Mechanical properties of nylon-6/SiO_2 nanofibers prepared by electrospinning. *Mater. Lett.* **63**, 34–36.

11. Zhang, D., A. B. Karki, D. Rutman, D. P. Young, A. Wang, D. Cocke, T. H. Ho, and Z. H. Guo. (2009). Electrospun polyacrylonitrile nanocomposite fibers reinforced with Fe_3O_4 nanoparticles: Fabrication and property analysis. *Polymer* **50**, 4189–4198.
12. Rangari, V. K., M. Y. Shaik, H. Mahfuz, and S. Jeelani. (2009). Fabrication and characterization of high strength nylon-6/Si_3N_4 polymer nanocomposite fibers. *Mater. Sci. Eng. A* **500**, 92–97.
13. Ji, L. W., A. J. Medford, and X. W. Zhang. (2009). Electrospun polyacrylonitrile/zinc chloride composite nanofibers and their response to hydrogen sulfide. *Polymer* **50**, 605–612.
14. Wang, L., Y. Yu, P. C. Chen, D. W. Zhang, and C. H. Chen. (2008). Electrospinning synthesis of C/Fe_3O_4 composite nanofibers and their application for high performance lithium-ion batteries. *J. Power Sources* **183**, 717–723.
15. Jang, J. W., J. H. Kim, and J. Y. Bae. (2005). Effects of Lewis acid-type transition metal chloride additives on the thermal degradation of ABS. *Polym. Degrad. Stab.* **88**, 324–332.
16. Jang, J. W., J. H. Kim, and J. Y. Bae. (2005). Synergistic effect of ferric chloride and silicon mixtures on the thermal stabilization enhancement of ABS. *Polym. Degrad. Stab.* **90**, 508–514.
17. Cai, Y. B., Y. Hu, L. Song, S. Y. Xuan, Y. Zhang, Z. Y. Chen, and W. C. Fan. (2007). Catalyzing carbonization function of ferric chloride based on acrylonitrile-butadiene-styrene copolymer/organophilic montmorillonite nanocomposites. *Polym. Degrad. Stab.* **92**, 490–496.
18. Zong, X. H., K. Kim, D. F. Fang, S. F. Ran, B. S. Hsiao, and B. Chu. (2002). Structure and process relationship of electrospun bioabsorbable nanofiber membranes. *Polymer* **43**, 4403–4412.
19. Son, W. K., J. H. Youk, T. S. Lee, and W. H. Park. (2004). The effects of solution properties and polyelectrolyte on electrospinning of ultrafine poly(ethylene oxide) fibers. *Polymer* **45**, 2959–2966.
20. Choi, J. S., S. W. Lee, L. Jeong, S. H. Bae, B. C. Min, and J. H. Youk. (2004). Effect of organosoluble salts on the nanofibrous structure of electrospun poly(3-hydroxybutyrate-co-3-hydroxyvalerate). *Int. J. Biol. Macromol.* **34**, 249–256.
21. Zhu, J., F. M. Uhl, A. B. Morgan, and C. A. Wilkie. (2001). Studies on the mechanism by which the formation of nanocomposites enhances thermal stability. *Chem. Mater.* **13**, 4649–4654.
22. Liu, J., Y. Hu, S. F. Wang, L. Song, Z. Y. Chen, and W. C. Fan. (2004). Preparation and characterization 6/Cu^{2+}-exchanged and Fe^{3+}-exchanged montmorillonite nanocomposite. *Colloid Polym. Sci.* **282**, 291–294.

Downloaded At: 15:21 21 January 2011